Journal of Applied Polymer Science

Dynamically Vulcanized Acrylonitrile-Butadiene-Styrene Terpolymer/Nitrile Butadiene Rubber Blends Compatibilized by Chlorinated Polyethylene

Dongya Wei, Jing Hua, Zhaobo Wang
College of Materials Science and Engineering, Qingdao University of Science and Technology, Qingdao 266042, People's Republic of China
Correspondence to: Z. Wang (E-mail: wangzhb.cn@gmail.com)

ABSTRACT: Thermoplastic vulcanizates (TPVs) based on acrylonitrile–butadiene–styrene (ABS)/nitrile butadiene rubber (NBR) blends were prepared by dynamic vulcanization and then compatibilized by chlorinated polyethylene (CM). The effects of CM compatibilizer on the mechanical properties, Mullins effect, and morphological and dynamic mechanical properties of the TPVs were investigated systematically. Experimental results indicated that CM had an excellent compatibilization effect on the dynamically vulcanized ABS/NBR TPVs. Mullins effect results showed that the compatibilized ABS/NBR TPV had relatively lower internal friction loss than the ABS/NBR TPV, indicating the improvement of elasticity. Morphology studies showed that the fracture surfaces of ABS/CM/NBR TPVs were relatively smoother, indicating the improved elastic reversibility. DMA studies showed that the glass to rubber transition temperatures of ABS and NBR phases were slightly shifted toward each other with the incorporation of CM compatibilizer, which indicates the improvement of the compatibility. © 2014 Wiley Periodicals, Inc. J. Appl. Polym. Sci. **2014**, *131*, 40986.

KEYWORDS: blends; viscosity and viscoelasticity; surfaces and interfaces

Received 26 November 2013; accepted 7 May 2014
DOI: 10.1002/app.40986

INTRODUCTION

Thermoplastic elastomers (TPEs) are rubbery materials that exhibit properties similar to those of conventional vulcanized rubbers but are processable at an elevated temperature; the thermoplastic vulcanizates (TPVs) are a special class of TPEs produced via dynamic vulcanization in the presence of a vulcanizing system.[1–3] Dynamic vulcanization was first described by Gessler[4] and then developed by Fisher,[5] Coran and Patel,[6] and Abdou-Sabet and Michael.[7] During dynamic valcanization, the rubber is vulcanized and finely dispersed in a continuous thermoplastic matrix with shear forces,[8] and the resulting materials exhibit outstanding mechanical properties and can be melted and recycled repeatedly. This technology led to a significant number of new TPE products commercialized during the mid- to late-1980s.[9]

Nitrile butadiene rubber (NBR) because of its excellent oil resistance has been used in a number of applications that include O-rings and oil hoses, and NBR had been used in a variety of blends by different authors as well. Tian et al.[10] investigated the influence of compatibility on crystallization behavior and morphology of polypropylene in PP/NBR TPVs. Fagundes and Jacobi[11] reported the influence of a crosslinked system on the morphology and properties of TPVs based on polyamide (PA)/NBR, and the effect of dynamic vulcanization on the properties and morphology of PA/SAN/NBR blends was also investigated.[12] Zhang et al.[13] studied the compatibility and physical properties of chlorinated polyethylene rubber (CM)/NBR blends. Acrylonitrile–butadiene–styrene (ABS) is widely used for industrial and domestic appliances because of its excellent mechanical properties, dimensional stability, and chemical resistance performances. López et al.[14] investigated the phase-separation behavior and morphologies of the blends of ABS with an epoxy/cycloaliphatic amine resin. Zhang et al.[15] reported the toughening modification of poly(vinyl chloride) (PVC)/α-methylstyrene–acrylonitrile–butadiene–styrene copolymer blends via adding CM. Blending ABS with NBR by dynamic vulcanization might be expected to yield a type of TPV, which combined the excellent processing characteristics of ABS and the excellent oil-resistant characteristics of NBR.

However, blends of thermoplastic and rubber are usually incompatible and may result in poor mechanical properties because of gross phase separation, poor interfacial adhesion, and lack of physical and chemical interactions. However, the further improvement of TPV properties can often be achieved by the addition of compatibility components, which can effectively

enhance the interfacial adhesion.[16–18] Block and graft copolymers have been extensively used in blend compatibilization, and the addition of a third polymer which is (partially) miscible with all blend phases is also interesting because it is often less expensive.[19] TPVs based on ABS and a variety of rubber (including NBR) were first reported by Coran et al.[20] Anandhan et al.[21] investigated the effects of blend ratio and dynamic vulcanization on the mechanical and morphology properties of the blends of NBR and scrap computer plastics (SCPs) based on ABS, and then they investigated the mechanical properties and recyclability of the SCPs with NBR and waste NBR powder.[22] However, to our knowledge, no reports on the compatibilization of dynamic vulcanizates based on the mixtures of ABS and NBR blends are available. CM was synthesized by randomly chlorinating the polyethylene backbone, resulting in a copolymer consisting of randomly distributed chlorinated blocks and ethylene segments.[23] CM had been used as a third component additive to compatibilize various blends, such as PA-reinforced ethylene propylene diene rubber (EPDM),[24] ethylene–vinyl acetate copolymer (EVA)/EPDM,[25] PVC/EPDM,[26] and NBR/EVA[17] blends. Therefore, it is beneficial to choose CM as compatibilizer to enhance the ABS–NBR interfacial interaction.

In this article, we report the preparation of TPVs based on blends of ABS and NBR via dynamic vulcanization, with the ABS–NBR interface compatibility being modified by the addition of CM compatibilizer. The influences of the compatibilizer on the mechanical properties, Mullins effect, and morphological and dynamic mechanical properties of the blends were investigated systematically.

EXPERIMENTAL

Materials

ABS copolymer [glass transition temperature (T_g) = 125°C], injection-grade EX18T, was supplied by UMG ABS, Japan, with a melt flow index of 14 g/10 min (230°C, 5.0 kg). NBR rubber [3305 type, with acrylonitrile content of 35 wt % and ML_{1+4}(100°C) =45] was commercially manufactured by Lanzhou Petrochemical, China. CM rubber, [grade 135, with chlorine content of 35 wt % and ML_{1+4}(125°C) =100] was commercially manufactured by Qingdao Hygain Chemical (Group), China. Sulfur, used as a vulcanizing agent, was obtained from Hengye Zhongyuan Chemical, China. *N*-Cyclohexyl-2-benzothiazole sulfenamide (CZ) and tetramethyl thiuram monosulfide (TS), used as accelerators, were manufactured by Northeast Auxiliary Chemical Industry, China. Zinc oxide (ZnO) was used as an activator and obtained from NewLe Qinshi Zinc, China. Stearic acid was also used as an activator and obtained from Wanyou, China. Poly(1,2-dihydro-2,2,4-trimethyl-quinoline) (Antioxidant RD) was used as an antioxidant and obtained from Shengao Chemical, China.

Preparation of Dynamically Vulcanized ABS/CM/NBR Blends

Commercially available ABS, NBR, and CM, as above, were used for the TPVs. The concentrations for crosslinking the NBR system are expressed in parts per hundred of NBR rubber by weight (phr). The sulfur-containing accelerating system recipe for crosslinking the NBR consisted of the following ingredients: 100 phr NBR, 1.0 phr sulfur, 1.5 phr CZ, 1.2 phr TS, 5.0 phr ZnO, 1.5 phr stearic acid, and 1.0 phr Antioxidant RD.

The dynamically vulcanized ABS/CM/NBR TPVs were produced via a two-step mixing process. In the first step, the preblends containing NBR and the crosslinking ingredients were compounded in a two-roll mill at room temperature. After 3 min of mixing time, the preblends were removed from the mixer. In the second step, the TPV compounds were prepared by melt-mixing the NBR preblends with ABS resins and CM rubber using a Brabender PLE 331 Plasticorder (Brabender Gmbh, Germany). The mixer temperature was kept at 160°C with a constant rotor (cam type) speed of 80 rpm. The ABS/NBR blending ratio was fixed at 35/65, and the CM amount was varied from 0 to 18 phr. The requisite quantities of ABS resin and CM were charged into the mixer and allowed to melt. After 3 min, the NBR-based preblend was added. The mixing was continued for another 8 min to allow the dynamic vulcanization. Finally, the compound was removed from the mixer and passed through a cold two-roll mill in the molten state to obtain a sheet. The sheet, about 2 mm thick, was compression-molded under a pressure of 15 MPa at 180°C for 5 min, followed by cold compression in another molding machine for 8 min at room temperature. Test specimens were die-cut from the compression-molded sheet and used for testing after 24 h.

Characterization

Mechanical Properties. For the measurement of tensile properties, dumbbell-shape specimens were prepared according to ASTM D-412. The tearing strength was tested according to ASTM D-624 using unnotched 90° angle test pieces. Both tensile and tearing tests were performed on a universal testing machine (TCS-2000; GoTech Testing Machines, China) at a crosshead speed of 500 mm/min. The average value of tensile strength was calculated for five test specimens and that of tearing strength was calculated for three test specimens. The Shore A hardness was determined using a hand-held Shore A Durometer (LX-A; Shanghai Liu Ling Instrument Factory, China) according to ASTM D-2240. All tests were carried out at 23°C. The tensile set at 100 % elongation was tested according to ASTM D1566-09. Firstly, the specimens were stretched to 100 % elongation, hold for 1 minute; then the specimens were removed from the testing machine, and the final length was measured after 1 minute. It is a definition, when the tensile set at 100 % elongation was less than 50 %, the material can be describe as a rubber-like elastomer; it can also represent the elastic recovery ability of a material under the same stretch.

Mullins Effect. To illustrate the material softening resulting from the Mullins effect, cyclic uniaxial tension tests were performed on ABS/NBR (35/65 weight ratio) and ABS/CM/NBR (35/6/65 weight ratio) TPVs. Flat tensile samples were cut from the compression-molded sheets. Uniaxial tension tests were performed on a TCS-2000 tensile machine (GoTech Testing Machines) operated in a local strain control mode. Tests were run at a low constant strain rate of 0.042 s^{-1}. For a given TPV sample, one sample was submitted to a simple uniaxial tension test, whereas another one was submitted to a cyclic uniaxial tension test with the maximum stretching increasing every five cycles. The stress–stretch curves during the loading and unloading period were measured. The maximum stress, residue deformation, internal friction, and degree of stress-softening effect

could be measured or calculated from the stress–stretch curves. The maximum stress values were the maximum stress of loading–unloading cycles under different stretches, namely, the values of stress corresponding to the maximum strain in each cycle. The residual deformation results were calculated according to the deformation remaining immediately after unloading period, namely, the values of strain in each cycle when the stress values fall to zero. The internal friction values were calculated by Origin 8.0 software (OriginLab Corporation) from the hysteresis rings of the stress–stretch curves, namely, the areas between loading–unloading cycle curves and *x*-axis in each cycle. The integral results of the strain energy were calculated by Origin 8.0 software, and the degree of stress-softening effect (D_s) can be expressed as follows[27]:

$$D_s = \frac{W_1(\varepsilon) - Wi(\varepsilon)}{W_1(\varepsilon)} \times 100\%, \quad (1)$$

where W_1 is the strain energy needed during the first loading for a given stretch and $W_i(\varepsilon)$ is the strain energy needed during the number of i loading for the given stretch, which was calculated by integrating the area that was surrounded by the horizontal axis and the stress–stretch curve during loading period.

Microscopy Analysis. Morphological study was carried out using field-emission scanning electron microscopy (FE-SEM; JEOL-6700F; Japan Electron, Japan). For the etched specimens, the ABS phase was extracted by immersing the blends into acetone for 120 min at room temperature, and then the etched samples were dried in vacuum oven at 30°C for 24 h. The etched surfaces and the fracture surfaces of the specimens were sputtered with thin layers of gold and imaged using FE-SEM.

Dynamic Mechanical Analysis. Dynamic mechanical analysis (DMA) of pure ABS, pure CM, and ABS/CM/NBR TPVs with various CM incorporations was measured with a dynamic mechanical thermal analysis system (EPLexor 500N; Gabo, Germany) in the tensile mode. The sample of the DMA has a width of 4 mm, a thickness of about 2 mm, and a length of 25 mm. The experiment was carried out over a temperature range of −60°C to 140°C with a programmed heating rate of 3°C/min at a frequency of 0.5 Hz and a strain of 1%, giving storage modulus E', loss modulus E'', and loss tangent tan δ. The temperature corresponding to the peak in tan δ versus temperature plot was taken as the T_g.

RESULTS AND DISCUSSION

Influence of CM on the Mechanical Properties of the Dynamically Vulcanized ABS/NBR TPVs

Figure 1 illustrates the stress–strain behaviors of the dynamically vulcanized 35/65 (weight ratio) ABS/NBR TPVs compatibilized by different CM dosages, and the mechanical properties results of ABS/CM/NBR TPVs are presented in Table I. The stress–strain curves of ABS/CM/NBR TPVs were similar in the shape of their curves. Initially, an obvious increase in tensile stress and modulus could be observed (for 10% strain). On further deformation, the slope of the curves decreased with the stress increasing almost linearly until fracture occurred. Moreover, it can be seen that the initial slope of the curves gradually decreased with an increasing CM incorporation. All the stress–strain curves showed the representative elastomeric character of being soft and tough, particularly at the higher loading levels of CM compatibilizer. From Figure 1, it can also be seen that the tensile strength and the elongation at break of ABS/CM/NBR TPVs were improved obviously when the dosage of CM compatibilizer was 15 phr below.

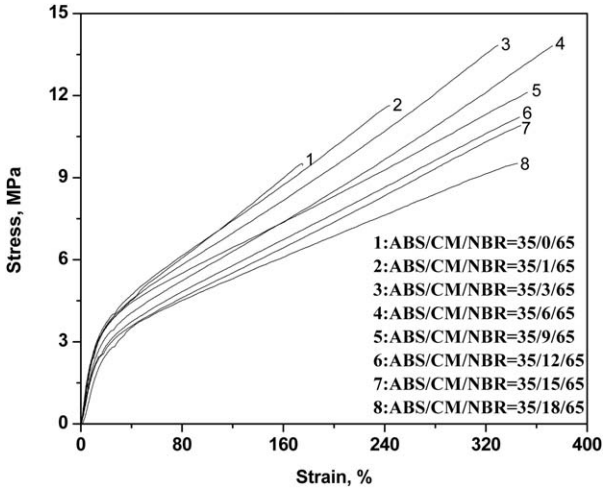

Figure 1. Stress–strain curves of dynamically vulcanized ABS/CM/NBR TPVs.

As shown in Table I, with the increasing of CM loading in the ABS/CM/NBR TPVs, the elongation at break improved significantly and reached a maximum value at 6 phr CM incorporation, increasing from 178% (at 0 phr CM) to 373% (at 6 phr CM). The influence of CM loading on the tensile set at break was similar to that of the elongation at break; the larger elongation at break led to the larger tensile set at break. However, all the tensile set (100% elongation) values in Table I were much lower than 50%, indicating that the dynamic vulcanized ABS/CM/NBR blends can be described as elastomers. With the increasing of CM loading, the tensile strength in Table I was also substantially improved, which was similar with the influence of CM content on the elongation at break, increasing from 9.5 MPa (at 0 phr CM) to 13.8 MPa (at 6 phr CM). However, when the content of CM was 18 phr above, the tensile strength was lower than that of ABS/NBR TPVs. The CM loading had almost no influence on the Shore A hardness of the TPVs. The incorporation of CM also affected the tearing strength. As shown in Table I, the tearing strength substantially increased with the CM content increasing, and the best performance was achieved with a CM concentration of 6 phr, indicating a remarkable reinforcing effect on the ABS/NBR TPVs.

Usually, in the presence of a compatibilizer at the interface of TPVs, the rubber phase can be finely dispersed and the interface interaction can be enhanced.[28] In our experiment, the improvement of the various mechanical properties of the TPVs was clearly due to the incorporation of the CM compatibilizer. Because ABS and NBR both contain the same units of acrylonitrile and butadiene, they can compatibilize to some extent. However, the CM has good compatibility effect because the polarity of CM is close to that of ABS and that of NBR, and the CM has excellent compatibility with both ABS and NBR.[13,15] During the dynamic vulcanization, the CM dispersed

Table I. Influence of CM Content on the Mechanical Properties of ABS/NBR TPVs

ABS/CM/NBR (weight ratio)	Tensile strength (MPa)	Elongation at break (%)	Tensile set at 100% elongation (%)	Tensile set at break (%)	Tearing strength (kN/m)	Shore A hardness
35/0/65	9.5 ± 0.16	178 ± 4.70	28 ± 0.98	35 ± 1.14	48.5 ± 1.20	83 ± 0.64
35/1/65	11.6 ± 0.12	244 ± 3.61	27 ± 1.02	40 ± 0.98	51.3 ± 1.16	83 ± 0.67
35/3/65	13.8 ± 0.21	329 ± 4.24	30 ± 1.28	59 ± 1.10	53.3 ± 1.09	83 ± 0.87
35/6/65	13.8 ± 0.28	373 ± 4.11	25 ± 0.99	61 ± 1.07	55.1 ± 0.88	83 ± 0.84
35/9/65	12.1 ± 0.33	353 ± 4.25	25 ± 1.23	62 ± 0.88	56.1 ± 1.01	82 ± 0.64
35/12/65	11.2 ± 0.21	346 ± 3.28	27 ± 0.87	61 ± 1.32	55.3 ± 0.99	82 ± 0.60
35/15/65	10.9 ± 0.19	348 ± 2.41	27 ± 1.12	55 ± 1.41	48.9 ± 1.04	82 ± 0.80
35/18/65	9.5 ± 0.16	345 ± 3.81	25 ± 1.01	50 ± 1.05	47.5 ± 0.87	81 ± 0.78

in the ABS matrix could penetrate into the vulcanized NBR phase to a certain extent, promoting the interpenetration of macromolecules. The existence of CM in the ABS/NBR blends enhances the compatibility and interface interaction of the blends, which is similar with the influence of CM on PA/EPDM,[24] EVA/EPDM,[25] PVC/EPDM,[26] and NBR/EVA[17] blends. With the enhanced interface interaction, more stress will transmit to the dispersed phase though the interface until fracture occurred, and the dispersed phase will undertake more stress accordingly; thus, a significant improvement of mechanical properties of TPVs will be observed with the incorporation of compatibilizer. Besides, the existence of compatibilizer decreases the interfacial energy and promotes mixing.[29] This leads to fine dispersed rubber particles and, in turn, increased the various mechanical properties of TPVs. When compared with that of the ABS/NBR TPVs, the tensile strength, elongation at break, and tearing strength of ABS/CM/NBR TPVs with only 6 phr CM incorporation were improved by about 45.3%, 109.6%, and 13.6%, respectively, indicating the remarkable influence on the improvement of interface interaction. Furthermore, the CM itself is an elastomer with relatively low Shore A hardness, and the presence of CM in the ABS continuous phase inevitably improves the plastic deformation ability of the ABS matrix, leading to the significant increase in the elongation at break.

Mullins Effect of ABS/NBR and ABS/CM/NBR TPVs

Usually, particle-filled rubbers are characterized by specific nonlinear mechanical behaviors including high hysteresis and stress softening (Mullins effect).[30] Mullins[27] wrote his review on the phenomenon; however, until now, no general agreement has been found either on the physical source or on the mechanical modeling of this effect.[31] Significant hysteresis illustrates the viscoelastic behavior; moreover, the hysteresis amount is a function of the maximum strain level and is more significant during the first cycles of each strain levels. Actually, the first cycle of each strain level is particular as they involve Mullins effect.[32]

Figure 2 illustrates the stress–stretch (L/L_0) curves of ABS/NBR and ABS/CM/NBR TPVs submitted to five uniaxial loading–unloading cycles with given stretch $\lambda = 1.5$, $\lambda = 2.0$, $\lambda = 2.5$, and $\lambda = 3.0$ (five cycles of loading–unloading from zero stress up to the maximum stretch down to zero stress). In Figure 2, during loading–unloading cycles, a slight softening phenomenon could be observed, which was characterized by a lower resulting stress for the same applied strain, appeared remarkably after the first loading. However, when the extension exceeded the maximum stretch previously applied, the stress–strain response followed the same return path as that of the monotonous uniaxial tension test, indicating that previous stretches had little influence on the stress–stretch properties at greater stretch.

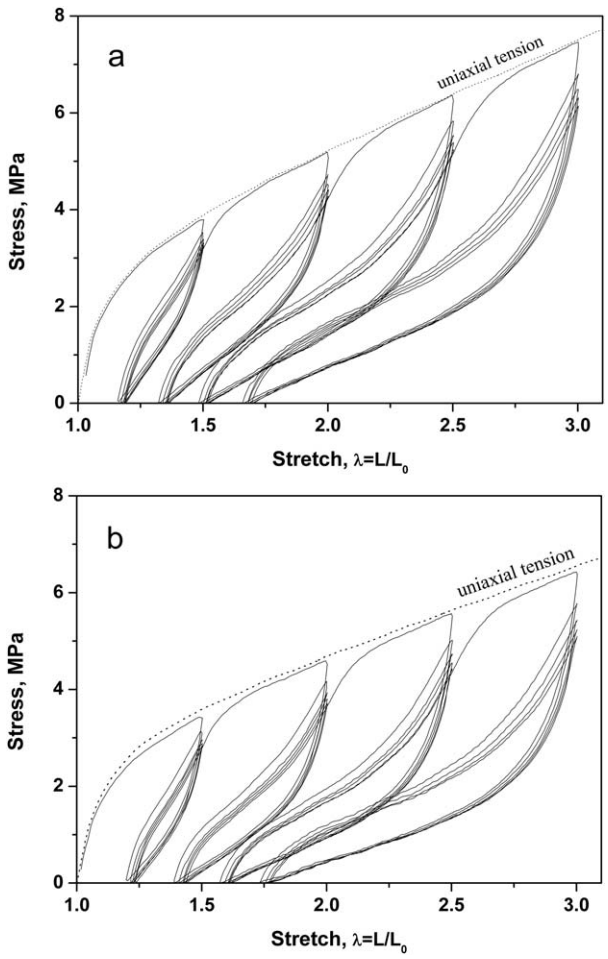

Figure 2. Stress–stretch responses of TPVs submitted to a simple uniaxial tension and to a cyclic uniaxial tension with increasing maximum stretch for every five cycles: (a) ABS/NBR = 35/65 and (b) ABS/CM/NBR = 35/6/65.

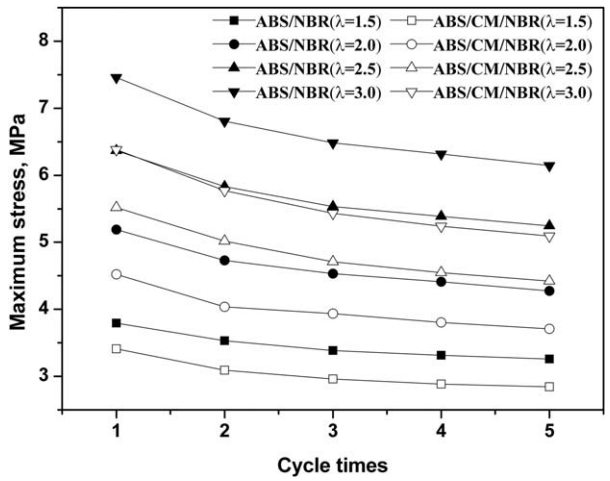

Figure 3. The maximum stress of ABS/NBR and ABS/CM/NBR TPVs as a function of the number of loading–unloading cycles.

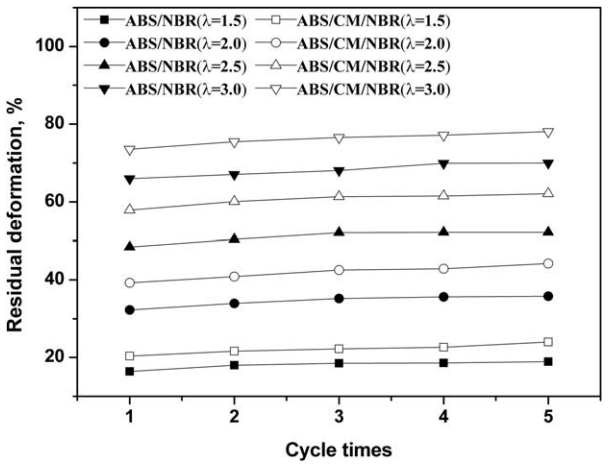

Figure 4. The residual deformation of ABS/NBR and ABS/CM/NBR TPVs as a function of the number of loading–unloading cycles.

Figure 3 shows the maximum stress values of ABS/NBR and ABS/CM/NBR TPVs of the loading–unloading cycles under different stretches. The stress decreased obviously after the first loading–unloading especially at high stretch; however, it only decreased slightly at the later loading–unloading cycles, and the lower stretch led to the slighter decrease of stress. The stress of ABS/CM/NBR TPV at a given stretch and loading–unloading cycle was lower than that of ABS/NBR TPV, which is consistent with the results in Figure 1. Nevertheless, the residual deformation results of the TPVs in uniaxial loading–unloading cycles, which were calculated according to the deformation remaining immediately after the unloading period, shown in Figure 4, were much higher than that due to the Mullins effect of conventional filled and unfilled vulcanizates.[33] Besides, the results of the residual deformations were increased with the increasing stretches while they were almost unchanged with the number of loading–unloading cycles. To characterize the uniaxial tensile behavior, Mullins and Tobin[34] proposed a microstructural model, the stress-softening virgin material contained a hard phase and a soft phase, most of the deformation occurs in the soft phase, and the extent of the damage depending on the maximum previous stretch experienced by the material. In our experiment, the ABS, as a hard phase, is the matrix of the TPVs. During the first loading–unloading, the plastic deformation and tearing strips of ABS matrix will generate and result in the large energy consumption and relatively high residual deformation; after the previous cycle, the contribution to the deformation of the hard region (matrix phase) is relatively small. During the follow-up loading–unloading cycles under the same stretch, most of the deformation takes place in the soft regions, the hard regions of ABS matrix make little contribution to the deformation, and the measured stress at a given strain is mainly exerted to the soft region. Therefore, the maximum stress and the residual deformation changed slightly at the later cycles after the first loading, as shown in Figures 3 and 4; however, the maximum stress and the residual deformation were increased with the increasing of stretch. It is easy to understand that large deformation needs large energy and will result in relatively high residual deformation.

To investigate the internal friction loss during the loading–unloading cycles, the integral results of the hysteresis rings were calculated by Origin 8.0 software; the results are shown in Figure 5. We can understand that the internal friction loss was increased obviously with the increasing stretches and that the maximum internal friction loss was generated in the first loading–unloading cycle under the specific stretch; however, the hysteresis loss in the second cycle was much lower than that of the first cycle and then only decreased slightly. It should be noted that the variation of internal friction loss was consistent with the variation of stress and residual deformation as shown above, and the large plastic deformation of ABS matrix during the first loading–unloading cycle results in the large hysteresis ring and residual deformation; however, during the later loading–unloading cycles, the measured stress at a given strain is mainly exerted to the soft region and the residual deformation was almost unchanged, leading to the lower internal friction loss. When compared with that of ABS/NBR TPV, the compatibilized ABS/NBR TPVs had the relatively lower internal friction loss for a specific stretch, indicating the improvement of elasticity.

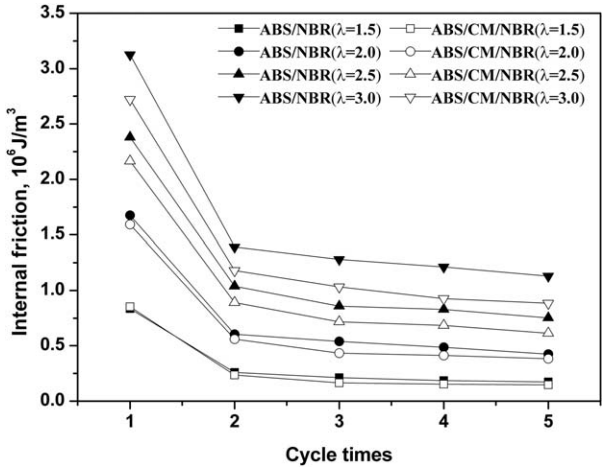

Figure 5. The internal friction of ABS/NBR and ABS/CM/NBR TPVs as a function of the number of loading–unloading cycles.

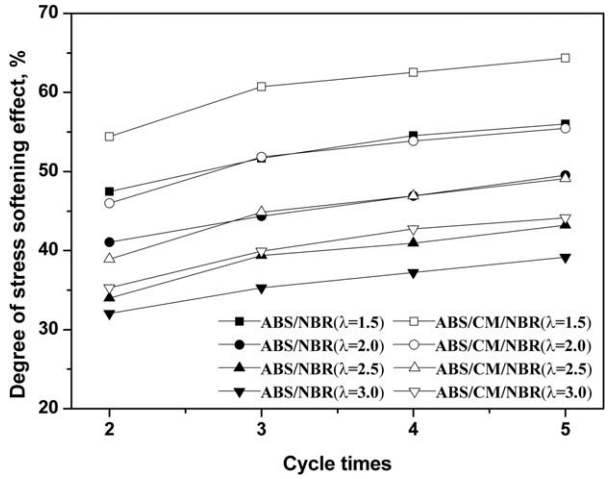

Figure 6. The degree of stress-softening effect of ABS/NBR and ABS/CM/NBR TPVs as a function of the number of loading–unloading cycles.

To illustrate more directly the difference of stress softening between ABS/NBR and ABS/CM/NBR TPVs, the D_s was calculated, and the results are shown in Figure 6. From Figure 6, it can be seen that when compared with that of ABS/NBR TPV, the ABS/CM/NBR TPV had the relatively higher degree of stress-softening effect for a specific stretch; moreover, the degrees of stress-softening effect were decreased with the increasing stretches, whereas they were increased slightly with the number of loading–unloading cycles. The D_s of ABS/CM/NBR TPV was higher than that of ABS/NBR TPV, which is probably due to the improvement of the plastic deformation ability of ABS matrix with CM loading. The more times the loading–unloading cycles at a given stretch, the softer will be the TPVs, resulting in the slightly increasing of the D_s for a specific stretch. During the previous stretches, partial plastic deformation had taken place, which would decrease the strain energy needed during the first loading for the later stretches, leading to the decrease of the D_s with the increasing stretches.

Morphology and Microstructure of ABS/CM/NBR TPVs

To study the relationship of the type of morphology with the mechanical properties, FE-SEM micrograph studies of the tensile fracture surfaces and etched surfaces of ABS/NBR and ABS/CM/NBR TPVs were carried out using FE-SEM. FE-SEM micrographs of the tensile fracture surfaces of ABS/CM/NBR blends prepared by dynamic vulcanization are shown in Figure 7. Figure 7(a) shows the morphology of ABS/NBR TPV without the incorporation of CM, used as a blank sample. In Figure 7(a), there are numerous lump structures with irregular shapes on fractured surface, which may caused by the residual deformation of the resin phase. For the TPV compatibilized with CM, the edges of the irregular structures on the surface were relatively smooth, as shown in Figure 7(b). The improved interface interaction of ABS/NBR TPV modified by the incorporation of compatibilizer, together with the improved elasticity of ABS matrix over pure ABS by the incorporation of CM, led to the enhanced deformation recoverability and interface interaction when compared with that of ABS/NBR TPV.

During the dynamic vulcanization, the viscosity of the NBR phase increased quickly because of the initiation of the crosslinking reaction, and then the NBR phase was gradually broken down into dispersed particles under the shear force. Figure 8 presents the etched surfaces of ABS/NBR and ABS/CM/NBR TPVs for which the ABS phases were etched from the sample surfaces to provide a better insight into the blend morphology. The vulcanized NBR domains remained undissolved and tended to merge during the swelling and deswelling. They are the current surfaces. As it can be seen from Figure 8(a), the crosslinked NBR particles, with irregular morphologies, were dispersed evenly in the thermoplastic matrix. The dimensions of the discrete NBR particles were in the range of 10–15 μm. When comparing ABS/CM/NBR TPV with ABS/NBR TPV, the presence of compatibilizer CM in matrix influenced the average size of the NBR particles slightly, as shown in Figure 8(b). It should be noted that, even though only 35% of the sample, the ABS would have formed the continuous phase before etching as the dynamically vulcanized ABS/CM/NBR blends were thermoplastic and could all be melted and molded repeatedly.

Dynamic Mechanical Properties of ABS/CM/NBR TPVs

DMA is often used to study polymer/polymer miscibility in polymer blends. The glass transition region can be studied using

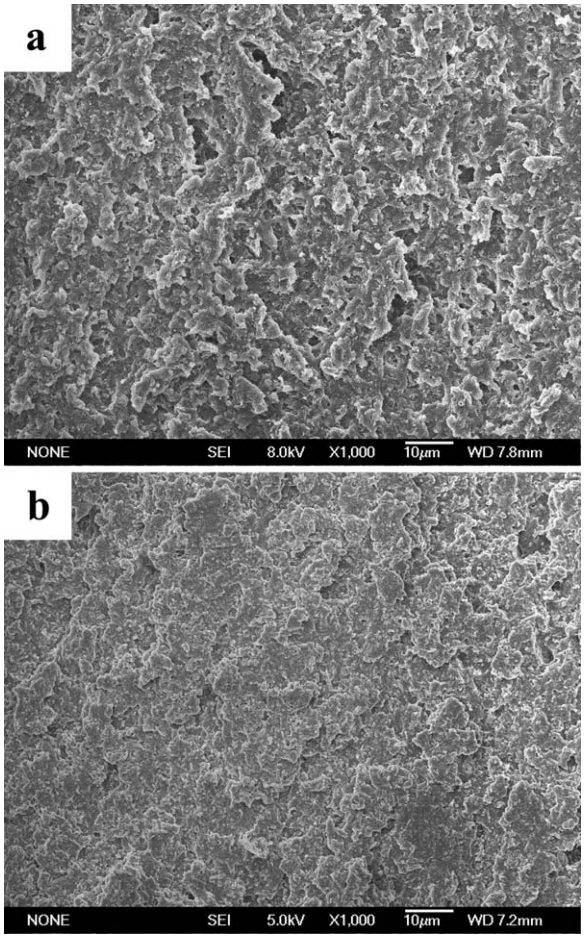

Figure 7. The fractured surfaces of the dynamically vulcanized ABS/CM/NBR TPVs: (a) ABS/NBR = 35/65 and (b) ABS/CM/NBR = 35/6/65.

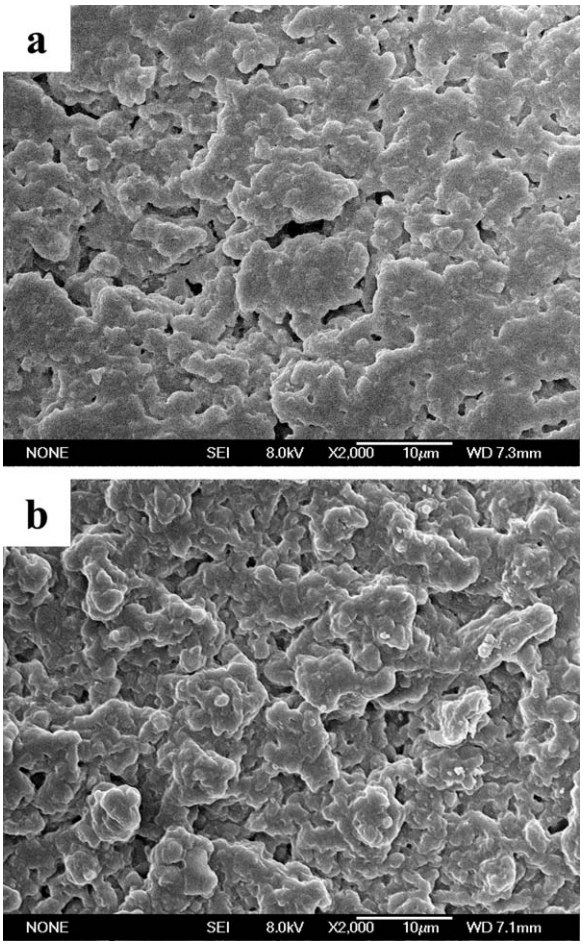

Figure 8. The FE-SEM of etched specimens of dynamically vulcanized ABS/CM/NBR TPVs: (a) ABS/NBR = 35/65 and (b) ABS/CM/NBR = 35/6/65.

loss factor (tan δ) curves. The results of DMA add information about the behavior of the blends and phase morphology. In the case of partially compatibilized polymer blends, two separate peaks corresponding to the individual polymer components can be observed, but with their position shifted to a higher or lower temperature depending on the compatibility of the blend composition and the influence of their microstructure.[35] Usually, in the presence of a compatibilizer at the interface of TPVs, the rubber phase can be finely dispersed and the interface interaction can be enhanced, which were verified by the improved mechanical properties and the T_gs of the two components shifting toward each other.[36] The viscoelastic behavior of pure ABS, pure CM, and ABS/CM/NBR TPVs versus temperature had been investigated, and the results are as below.

The temperature dependence of the storage modulus (E') and loss modulus (E'') of pure ABS, pure CM, and ABS/CM/NBR TPVs with various CM contents are shown in Figure 9, respectively. From Figure 9, we can see that the E' of ABS/CM/NBR TPVs was highest at low temperature and then decreased obviously to a lower value at about −15°C and 125°C. The loss modulus curves of ABS/CM/NBR TPVs in Figure 9 shows the similar variation while the values were much lower than that of storage modulus. All the storage modulus and loss modulus

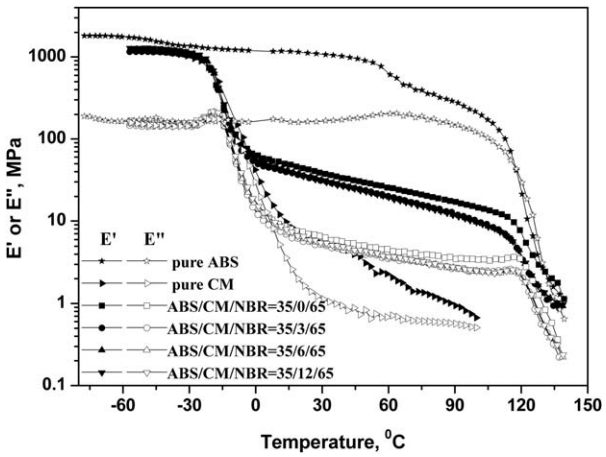

Figure 9. The temperature dependence of storage modulus (E') and loss modulus (E'') of pure ABS, pure CM, and ABS/CM/NBR TPVs with various CM incorporations.

curve values of ABS/CM/NBR TPVs were lower than that of pure ABS.

Figure 10 shows the temperature dependence of loss factor of pure ABS, pure CM, and ABS/CM/NBR TPVs with various CM incorporations; to observe the shift more clearly, the images close to the peak were partially enlarged. As we can see from Figure 10, two major peaks around −15°C and 125°C can be noticed in tan δ versus temperature plot of ABS/CM/NBR TPVs, which corresponded to the T_g of the NBR and ABS phases, respectively. The temperatures corresponding to the maximum peak related to the NBR and ABS transition were slightly shifted toward each other with the incorporation of CM compatibilizer, which indicates the improvement of the compatibility; therefore, the mechanical properties were improved significantly because of the enhanced interface interaction. Usually, the T_g of the compatibilizer is between the T_gs of the two components, and the compatibility of composites was improved when the T_gs of the two components are shifted toward each other. In the experiments, the T_g of CM is between that of ABS and that of NBR which is beneficial for the compatibility of

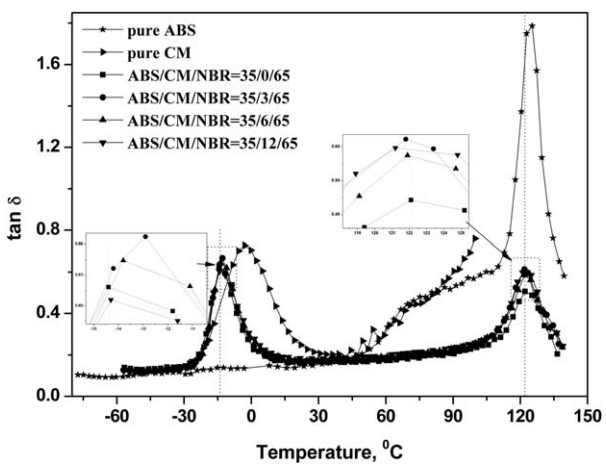

Figure 10. The temperature dependence of loss factor (tan δ) of pure ABS, pure CM, and ABS/CM/NBR TPVs with various CM incorporations.

CM compatibilizer; the CM was incorporated into ABS matrix during mixing process as a compatibilizer, and the T_g of CM rubber was much lower than that of ABS. Therefore, the peak corresponded to the T_g of the ABS phase somewhat moved toward lower temperature. However, the chain segments of CM dispersed in the ABS matrix could penetrate into the vulcanized NBR phase to a certain extent during the dynamic vulcanization, which would inevitably improve the interface interaction between the ABS and NBR phases and lead to the increasing of the T_g of NBR phase.

CONCLUSIONS

TPVs based on ABS/NBR were prepared by melt-mixing. Dynamic vulcanization of the blends was performed via a conventional sulfur vulcanization system and CM rubber as a compatibilizer. When compared with ABS/NBR TPV, significant improvement of mechanical properties of TPVs compatibilized by CM was achieved; the tensile strength and elongation at break reached a maximum at a compatibilizer resin content of only 6 phr. The Mullins effect results showed that the compatibilized ABS/NBR TPV had relatively lower internal friction loss than ABS/NBR TPV, indicating the improvement of elasticity. Morphology studies showed that the vulcanized NBR particles with irregular shape were dispersed evenly in the thermoplastic matrix, and the fracture surface of ABS/CM/NBR TPVs was relatively smoother than that of ABS/NBR TPV, indicating improved elastic reversibility. DMA studies showed that the T_gs of ABS and NBR phases were slightly shifted toward each other with the incorporation of CM compatibilizer, which indicates the improvement of the compatibility.

ACKNOWLEDGMENTS

This work was funded by the Shandong Provincial Natural Science Foundation, China (ZR2012EMM002; ZR2011EL008), a Project of Shandong Province Higher Educational Science and Technology Program (J12LA15), the Science and Technology Development Project of Qingdao [12-1-4-3-(9)-jch;13-1-4-133-jch], and the National Natural Science Foundation of China (51272115).

REFERENCES

1. Kalkornsurapranee, E.; Nakason, C.; Kummerlöwe, C.; Vennemann, N. *J. Appl. Polym. Sci.* **2013**, *128*, 2358.
2. Nicolini, A.; de Campos Rocha, T. L. Á.; Maldaner Jacobi, M. A. *J. Appl. Polym. Sci.* **2008**, *109*, 3093.
3. Razmjooei, F.; Naderi, G.; Bakhshandeh, G. *J. Appl. Polym. Sci.* **2012**, *124*, 4864.
4. Gessler, A. M.; Haslett, W. H. U.S. Pat. 3,037,954 (1962).
5. Fischer, W. K. U.S. Pat. 3,758,643 (1973).
6. Coran, A. Y.; Patel, R. *Rubber Chem. Technol.* **1980**, *53*, 141.
7. Abdou-Sabet, S.; Michael, A. F. U.S. Pat. 4,311,628 (1982).
8. Duin, M. V. *Macromol. Symp.* **2006**, *233*, 11.
9. Coran, A. Y.; Patel, R. *Rubber Chem. Technol.* **1983**, *56*, 1045.
10. Tian, M.; Han, J. B.; Zou, H.; Tian, H. C.; Wu, H. G.; She, Q. Y.; Chen, W. Q.; Zhang, L. Q. *J. Polym. Res.* **2012**, *19*, 1.
11. Fagundes, E.; Jacobi, M. A. M. *J. Appl. Polym. Sci.* **2012**, *123*, 3072.
12. Wang, Z. J.; Zhang, X. F.; Zhang, Y.; Zhang, Y. X.; Zhou, W. *J. Appl. Polym. Sci.* **2003**, *87*, 2057.
13. Zhang, Z. X.; Chen, C. H.; Gao, X. W.; Kim, J. K.; Xin, Z. X. *J. Appl. Polym. Sci.* **2011**, *120*, 1180.
14. López, J.; Ramirez, C.; Abad, M. J.; Barral, L.; Cano, J.; Diez, F. J. *J. Appl. Polym. Sci.* **2002**, *85*, 1277.
15. Zhang, Z.; Zhang, J.; Liu, H. *Polym. Eng. Sci.* **2014**, *54*, 378.
16. Lee, S. H.; Shanmugharaj, A. M.; Sridhar, V.; Zhang, Z. X.; Kim, J. K. *Polym. Adv. Technol.* **2009**, *20*, 620.
17. Li, S.; Liu, T.; Wang, L. J.; Wang, Z. B. *J. Macromol. Sci. Phys.* **2013**, *52*, 13.
18. Wang, Z. B.; Zhao, H. L.; Zhao, J.; Wang, X. *J. Macromol. Sci. Phys.* **2010**, *50*, 51.
19. Setua, D. K.; Pandey, K. N.; Saxena, A. K.; Mathur, G. N. *J. Appl. Polym. Sci.* **1999**, *74*, 480.
20. Coran, A. Y.; Patel, R. P.; Williams, D. *Rubber Chem. Technol.* **1982**, *55*, 116.
21. Anandhan, S.; De, P. P.; De, S. K.; Bhowmick, A. K.; Bandyopadhyay, S. *Rubber Chem. Technol.* **2003**, *76*, 1145.
22. Anandhan, S.; Bhowmick, A. K. *J. Mater. Cycles Waste Manage.* **2013**, *15*, 300.
23. Hu, X.; Zeng, J.; Dai, W. J.; Shi, W. Y.; Li, L.; Han, C. Y. *Polym. Bull.* **2011**, *66*, 703.
24. Liu, X.; Huang, H.; Zhang, Y.; Zhang, Y. X. *J. Appl. Polym. Sci.* **2003**, *89*, 1727.
25. Liu, C. P.; Lin, J. H. *J. Appl. Polym. Sci.* **2007**, *106*, 897.
26. Lee, Y. D.; Chen, C. M. *J. Appl. Polym. Sci.* **1987**, *33*, 1231.
27. Mullins, L. *Rubber Chem. Technol.* **1969**, *42*, 339.
28. Liu, X.; Huang, H.; Xie, Z. Y.; Zhang, Y.; Zhang, Y. X.; Sun, K.; Min, L. N. *Polym. Test.* **2003**, *22*, 9.
29. Shi, Q.; Stagnaro, P.; Cai, C. L.; Yin, J. H.; Costa, G.; Turturro, A. *J. Appl. Polym. Sci.* **2008**, *110*, 3963.
30. Harwood, J. A. C.; Mullins, L.; Payne, R. *J. Appl. Polym. Sci.* **1965**, *9*, 3011.
31. Diani, J.; Fayolle, B.; Gilormini, P. *Eur. Polym. J.* **2009**, *45*, 601.
32. Diani, J.; Brieu, M.; Vacherand, J. M. *Eur. J. Mech. A: Solids* **2006**, *25*, 483.
33. Dargazany, R.; Itskov, M. *Int. J. Solids Struct.* **2009**, *46*, 2967.
34. Mullins, L.; Tobin, N. R. *Rubber Chem. Technol.* **1957**, *30*, 555.
35. Al-Malaika, S.; Kong, W. *Polymer* **2005**, *46*, 209.
36. Jansen, P.; Garcia, F. G.; Soares, B. G. *J. Appl. Polym. Sci.* **2003**, *90*, 2391.